HHS Public Access

Author manuscript

Semin Thorac Cardiovasc Surg. Author manuscript; available in PMC 2017 April 01.

Published in final edited form as:

Semin Thorac Cardiovasc Surg. 2016 ; 28(1): 120–126. doi:10.1053/j.semtcvs.2015.12.015.

CANARY Risk Management of Adenocarcinoma: The Future of Imaging?

Finbar Foley, MD, MPH[a], **Srinivasan Rajagopalan, PhD**[b], **Sushravya M Raghunath, PhD**[c], **Jennifer M Boland, MD**[d], **Ronald A. Karwoski, BA**[e], **Fabien Maldonado, MD**[f], **Brian J Bartholmai, MD**[g], and **Tobias Peikert, MD**[h]

[a] Department of Pulmonary and Critical Care Medicine, Mayo Clinic, Rochester, MN

[b] Department of Radiology, Mayo Clinic College of Medicine, Rochester, MN

[c] Department of Radiology, Mayo Clinic College of Medicine, Rochester, MN

[d] Department of Pathology, Mayo Clinic, Rochester, MN

[e] Biomedical Imaging Resource, Mayo Clinic, Rochester, MN

[f] Division of Allergy, Pulmonary, and Critical Care Medicine, Vanderbilt University Medical Center, Nashville, Tennessee

[g] Department of Radiology, Mayo Clinic, Rochester, MN

[h] Department of Pulmonary and Critical Care Medicine, Mayo Clinic, Rochester, MN

Abstract

Increased clinical utilization of chest high resolution computed tomography results in increased identification of lung adenocarcinomas and persistent sub-solid opacities. However, these lesions range from very indolent to extremely aggressive tumors. Clinically relevant diagnostic tools to non-invasively risk stratify and guide individualized management of these lesions are lacking. Research efforts investigating semi-quantitative measures to decrease inter- and intra-rater variability are emerging, and in some cases steps have been taken to automate this process. However, many such methods currently are still sub-optimal, require validation and are not yet clinically applicable. The Computer-Aided Nodule Assessment and Risk Yield (CANARY) software application represents a validated tool for the automated, quantitative, non-invasive tool for risk stratification of adenocarcinoma lung nodules. CANARY correlates well with consensus histology and post-surgical patient outcomes and therefore may help to guide individualized patient management e.g. in identification of nodules amenable to radiological surveillance, or in need of adjunctive therapy.

Corresponding Author: Tobias Peikert, peikert.tobias@mayo.edu, Address: Gonda Building18 South, Division of Pulmonary and Critical Care Medicine, 200 First Street SW, Rochester, MN 55905, Phone: 507-284 4162, Fax: 507-266-4372.

Keywords

Lung adenocarcinoma; Risk stratification; Quantitative image analytics; Lung cancer screening; Pulmonary nodule

Introduction

The widespread implementation of low-dose high-resolution computed tomography (HRCT) based lung cancer screening is expected to reduce lung cancer mortality. (1) However, increased use of diagnostic and screening chest HRCT will also lead to the detection of an increased number of lung adenocarcinoma spectrum lesions ranging from indolent to very aggressive tumors. Approximately 15-20% of screen-detected cancers, mostly lung adenocarcinomas, are likely to be clinically inconsequential (overdiagnosed). (2) Comprehensive post-surgical histological assessment based on the updated IASLC lung adenocarcinoma classification can accurately risk-stratify these patients into indolent (adenocarcinoma in situ (AIS) / minimally invasive adenocarcinoma (MIA)) and aggressive lesions (invasive adenocarcinoma (IA)) (3). However, effective strategies for non-invasive, pre-treatment risk stratification are lacking. These tools are urgently needed to facilitate the individualized management of this increasing patient population to avoid overtreatment, iatrogenic morbidity, mortality and limit health care costs.

Radiologically, lung adenocarcinomas most commonly present as persistent sub-solid opacities ranging from pure ground glass to almost entirely solid lesions. (4-6) While ground glass areas typically correspond to lepidic growth, consolidation usually represent invasion, scarring and atelectasis.(7-9) Currently, clinical treatment decisions are largely based on the gestalt (pure ground glass = indolent, significant/increasing solid component = concern for invasion) of these lesions on single time point or serial HRCT imaging. (10) However, this practice is subjective and limited by intra- and inter-observer variability. In order to improve this approach, several investigators have used more quantitative measures including semi-quantitative assessment of the ratio of solid and ground glass components of lesions - for example, the two-dimensional consolidation to tumor (C/T) ratio (11-14), tumor shadow disappearance rate (15), or tumor histogram peak analysis (16). Pulmonary nodules with a low C/T ratio (< 0.25) have been linked to AIS/MIA histology and favorable patient outcomes (14), and fully automated methods to segment the solid and non-solid portions are being developed. (17) However, despite the fact that the C/T ratio has been used to identify candidates for limited versus standard surgical resection (18,19), none of these approaches are routinely used in clinical practice.

Several groups are developing techniques involving three-dimensional nodule segmentation and quantitative analysis. Scholten et al. described a semi-automated method to segment the solid and nonsolid components of pulmonary nodules. But this approach has not yet been validated or correlated with histology or clinical outcomes. (20) Son et al performed manual nodule segmentation through contiguous HRCT slices, and subsequently determined histogram and textural features that may differentiate AIS/MIA from IA nodules. Though they observed some differences in survival between these groups, the differences were not

clinically significant (21). Balagurunathan et al. employed both manual and automated nodule segmentation techniques, and analyzed both texture and non-texture (size, shape, location) factors. After determining the features which were reproducible, non-redundant, and aided in radiologic prognosis discrimination, they applied their model to a separate cohort of adenocarcinoma patients. The patients were dichotomized based on the model, yielding a difference in survival between the two groups in a small patient sample (n=59). (22) Yanagawa et al. described a method using semi-automated nodule segmentation followed by automated assessment of solid and ground glass components, and determined that nodule volume and the proportion of the solid component could be used to risk stratify patients. (23) Chae et al. derived an artificial neural network model based on textural features computed from manually segmented nodules to discriminate preinvasive (atypical adenomatous hyperplasia (AAH) and AIS) lesions from invasive. (24) Most recently, Li and colleagues investigated the C/T relationship and the average radiological density in a three-dimensional fashion by measuring the tumor volume, reconstructing nodules using an automated diagnostic system and automatically computing the overall and solid tumor volumes (25). Their training set allowed the identification of three risk groups for patients with clinical Stage IA lung adenocarcinoma. However, most of these promising results are limited by smaller datasets, a lack of validation, and robust correlation to clinically significant outcomes. The ultimate goal remains to create an automated segmentation and analysis system that can reduce measurement variability, correlates with histological measures of invasion, and has been independently validated to predict clinical outcomes.

CANARY-Based Risk Stratification

The **C**omputer **A**ided **N**odule **A**ssessment and **R**isk **Y**ield (CANARY) software developed at the Biomedical Imaging Resource, Mayo Clinic by a multidisciplinary team of scientists and physicians facilitates semi-automated segmentation and fully automated quantitative analysis and risk stratification of HRCT-based pulmonary nodules of the lung adenocarcinoma spectrum. (26) CANARY characterizes operator identified pulmonary nodules by summarizing voxel by voxel radiological tissue density based on the relative distribution of nine representative texture exemplars (texemes) within each lesion. The resulting CANARY nodule signatures correlate extremely well with the degree of tissues invasion based on consensus histopathology as assessed by three independent pulmonary pathologists. (27) The nine CANARY texture exemplars were identified through unsupervised clustering of 774 (9×9 voxel) arbitrarily selected regions of interest (ROI) across the spectrum of 37 known lung adenocarcinoma lesions. (**Figure 1A**) The nine identified texemes color coded as violet (V), indigo (I), blue (B), green (G), yellow (Y), orange (O), red (R), cyan (C) and pink (P) represent the building blocks of the CANARY nodule signature. . When processing a lung nodule, CANARY inspects each voxel and its 9×9 surrounding to compute the similarity to each of the 9 texemes, and the color code of the most similar texeme is ultimately assigned to the voxel. This process yields a unique color code for each nodule which can be displayed as a glyph representing the CANARY nodule signature. (**Figure 1B**) The user interface for the CANARY application is shown in **Figure 2**.

Comparison of pre-surgical HRCT based CANARY nodule signatures with consensus histology of the resected lesions demonstrated that the presence of V-I-R-O and B-C-G exemplars corresponds to histological tissue invasion and lepidic growth, respectively. (**Figure 3 and 4**) The relative distribution of V-I-R-O and B-C-G within pulmonary nodules of the lung adenocarcinoma spectrum correlated strongly with the degree of histopathological tissue invasion in a training set of lung nodules and was confirmed in an independent validation set (Spearman R=0.89, [0.83-0.93], $p < 0.001$). (27) This approach allows the accurate non-invasive, pre-surgical classification of lung nodules of the adenocarcinoma spectrum as AIS/MIA ("indolent") or IA ("aggressive") – in essence a "*radiological biopsy*". (**Figure 3**) Compared to consensus histopathology, CANARY's diagnostic performance was excellent demonstrating a sensitivity of 95.4% [95% CI 75.1–99.7%] and specificity of 96.8% [95% CI 82–99.8%], and a sensitivity of 98.7% [95% CI 91.8–99.9%] and specificity of 63.6% [95% CI 31.6–87.6%] in the training and independent validation set, respectively. Importantly, none of the patients characterized as "indolent" in either the training or validation set had locally advanced or metastatic disease. (27)

CANARY's nodule classification compared favorably with the assessment of "indolent" versus "aggressive" by expert thoracic radiologists. The two radiologists both correctly classified 36/54 nodules, disagreed with each other for 10/54, and misclassified 8/54 nodules compared with consensus histology. (κ 0.49, 95% CI: 0.21–0.78). Among the misclassified cases, seven of the eight cases were misclassified as aggressive while only one was misclassified as indolent. Next, a semi-quantitative measurement was incorporated to evaluate the change in agreement and accuracy. Using the two-dimensional C/T ratio of ≤0.25 to assist in nodule classification resulted in better agreement (κ = 0.78 (95% CI: 0.60–0.96)), with an average sensitivity of 91% (95% CI: 74–98%) and a specificity of 55% (95% CI: 33–75%) to detect invasion. (27) However, despite this improvement, the approach was still less sensitive and specific compared with CANARY, and remains subject to intra- and inter-rater variability.

While non-invasive prediction of histology is important, histology itself is a surrogate marker of patient outcomes and histologic assessment is subject to sampling error and inter-observer variability. In contrast, computer aided analysis permits a comprehensive and reproducible assessment of the entire lesion, and may represent an independent marker for outcomes. Consequently, we investigated the automatic identification of "natural" clusters of pulmonary nodules of the lung adenocarcinoma spectrum independent of histology. (28) CANARY nodule signatures were obtained for a cohort of 264 consecutive Mayo Clinic patients with available pre-operative HRCT and a diagnosis of lung adenocarcinoma based on surgical resection of a clinical Stage I solitary pulmonary nodule. All nodules were segmented and analyzed using CANARY, with investigators blinded to clinical patient outcomes. Initial analysis used 170 adenocarcinoma nodules. Unsupervised clustering of the exemplar distributions yielded three natural clusters which, when matched with disease free survival (DFS) information, demonstrated good (G), intermediate (I) and poor (P) prognosis groups. This analysis was confirmed using all 264 cases. Kaplan-Meier curves plotted for the G, I and P groups, showed 100%, 72.7%, and 51.4% 5-year DFS, respectively. Hazard ratio (HR) for 5-year DFS between nodules were significant: P vs G nodules (HR 5.338;

95% confidence limits 2.23-12.78; P = 0.0002); and I vs G nodules (HR, 3.47; 95% confidence limits, 1.44-8.22; P = 0.0055). (28)

Most recently, we independently validated this approach by analyzing all eligible lung adenocarcinoma cases (n=294) diagnosed by low-dose HRCT during the National Lung Screening Trial (NLST). (26) The investigators, blinded to the clinical outcome, generated CANARY nodule signatures for all the cases based on the last screening low-dose CT scan prior to the diagnosis of lung adenocarcinoma Based on the similarity between the "exemplar" nodules and the candidate nodules, all the lesions were classified as good, intermediate or poor risk.

Lung-cancer progression-free survival (PFS) was determined for all patients. Of the 294 subjects analyzed, 86 experienced recurrence or lung cancer-related death. Kaplan-Meier analysis validated distinct progression-free survival curves between the three CANARY risk groups (G, I and P) and this relationship was also present when the analysis was limited to all pathological stage I cases. Adjusted Cox regression analysis yielded statistically different HRs for PFS comparing P vs G cases (HR, 11.11; 95% confidence limits, 1.43-100; P = 0.02) and I vs G cases (HR, 8.33; 95% confidence limits, 1.15-50; P = 0.04). The 39 (18%) patients classified as CANARY-G among all Stage I patients (n=218) had a 100% progression-free survival. (26) CANARY correlation with PFS for the combined Mayo Clinic and NLST datasets is shown in **Figure 5**.

Conclusion

Validated and clinically applicable non-invasive pre-treatment risk stratification strategies are needed to individualize the treatment approach for the increasing number of patients discovered to have either biopsy proven or radiologically suspected (persistent sub-solid opacity) lesions of the lung adenocarcinoma. CANARY can reliably predict histological tissue invasion and represents a validated approach to robustly risk stratify these lesions into good (G), intermediate (I) and poor (P) risk groups. The lack of post-treatment disease recurrence in the CANARY G group suggests that these lesions may be overdiagnosed and potentially lend themselves to serial radiological surveillance (watchful waiting). However, this approach will require prospective validation. It is certainly possible that the favorable outcomes of some of these patients in our current series were impacted by surgical resections and other therapeutic interventions. In addition, we are in the process of characterizing the temporal evolution of CANARY G lesions over time in relationship to their clinical outcomes in an effort to identify the optimal juncture for an intervention. Furthermore, it is possible that patients with Stage I CANARY P lesions would benefit from adjuvant therapy. We are currently in the process of designing a prospective study to test this hypothesis. Ultimately, we believe that non-invasive automated quantitative image analysis techniques such as CANARY, validated to correlate to relevant clinical outcomes, represent the future in imaging.

References

1. Aberle DR, Adams AM, Berg CD, Black WC, Clapp JD, Fagerstrom RM, Gareen IF, Gatsonis C, Marcus PM, Sicks JD. National Lung Screening Trial Research Team. Reduced lung-cancer

mortality with low-dose computed tomographic screening. N Engl J Med. 2011; 365:395–409. [PubMed: 21714641]

2. Patz EF Jr, Pinsky P, Gatsonis C, Sicks JD, Kramer BS, Tammemagi MC, Chiles C, Black WC, Aberle DR. NLST Overdiagnosis Manuscript Writing Team. Overdiagnosis in low-dose computed tomography screening for lung cancer. JAMA Intern Med. 2014; 174:269–274. [PubMed: 24322569]
3. Travis WD, Brambilla E, Noguchi M, Nicholson AG, Geisinger KR, Yatabe Y, Beer DG, Powell CA, Riely GJ, Van Schil PE, Garg K, Austin JH, Asamura H, Rusch VW, Hirsch FR, Scagliotti G, Mitsudomi T, Huber RM, Ishikawa Y, Jett J, Sanchez-Cespedes M, Sculier JP, Takahashi T, Tsuboi M, Vansteenkiste J, Wistuba I, Yang PC, Aberle D, Brambilla C, Flieder D, Franklin W, Gazdar A, Gould M, Hasleton P, Henderson D, Johnson B, Johnson D, Kerr K, Kuriyama K, Lee JS, Miller VA, Petersen I, Roggli V, Rosell R, Saijo N, Thunnissen E, Tsao M, Yankelewitz D. International association for the study of lung cancer/american thoracic society/european respiratory society international multidisciplinary classification of lung adenocarcinoma. J Thorac Oncol. Feb; 2011 6(2):244–85. [PubMed: 21252716]
4. Zwirewich CV, Vedal S, Miller RR, Müller NL. Solitary pulmonary nodule: high-resolution CT and radiologic-pathologic correlation. Radiology. May; 1991 179(2):469–76. [PubMed: 2014294]
5. McWilliams A, Tammemagi MC, Mayo JR, Roberts H, Liu G, Soghrati K, Yasufuku K, Martel S, Laberge F, Gingras M, Atkar-Khattra S, Berg CD, Evans K, Finley R, Yee J, English J, Nasute P, Goffin J, Puksa S, Stewart L, Tsai S, Johnston MR, Manos D, Nicholas G, Goss GD, Seely JM, Amjadi K, Tremblay A, Burrowes P, MacEachern P, Bhatia R, Tsao MS, Lam S. Probability of cancer in pulmonary nodules detected on first screening CT. N Engl J Med. Sep 5; 2013 369(10): 910–9. [PubMed: 24004118]
6. Lee HY, Jeong JY, Lee KS, Kim HJ, Han J, Kim BT, Kim J, Shim YM, Kim JH, Song I. Solitary pulmonary nodular lung adenocarcinoma: correlation of histopathologic scoring and patient survival with imaging biomarkers. Radiology. Sep; 2012 264(3):884–93. [PubMed: 22829686]
7. Kuriyama K, Seto M, Kasugai T, Higashiyama M, Kido S, Sawai Y, Kodama K, Kuroda C. Ground-glass opacity on thin-section CT: value in differentiating subtypes of adenocarcinoma of the lung. AJR Am J Roentgenol. Aug; 1999 173(2):465–9. [PubMed: 10430155]
8. Kodama K, Higashiyama M, Yokouchi H, Takami K, Kuriyama K, Mano M, Nakayama T. Prognostic value of ground-glass opacity found in small lung adenocarcinoma on high-resolution CT scanning. Lung Cancer. Jul; 2001 33(1):17–25. [PubMed: 11429192]
9. Suzuki K, Asamura H, Kusumoto M, Kondo H, Tsuchiya R. "Early" peripheral lung cancer: prognostic significance of ground glass opacity on thin-section computed tomographic scan. Ann Thorac Surg. Nov; 2002 74(5):1635–9. [PubMed: 12440622]
10. Naidich DP, Bankier AA, MacMahon H, Schaefer-Prokop CM, Pistolesi M, Goo JM, Macchiarini P, Crapo JD, Herold CJ, Austin JH, Travis WD. Recommendations for the management of subsolid pulmonary nodules detected at CT: a statement from the Fleischner Society. Radiology. Jan; 2013 266(1):304–17. [PubMed: 23070270]
11. Ohde Y, Nagai K, Yoshida J, Nishimura M, Takahashi K, Suzuki K, Takamochi K, Yokose T, Nishiwaki Y. The proportion of consolidation to ground-glass opacity on high resolution CT is a good predictor for distinguishing the population of non-invasive peripheral adenocarcinoma. Lung Cancer. Dec; 2003 42(3):303–10. [PubMed: 14644518]
12. Matsuguma H, Nakahara R, Anraku M, Kondo T, Tsuura Y, Kamiyama Y, Mori K, Yokoi K. Objective definition and measurement method of ground-glass opacity for planning limited resection in patients with clinical stage IA adenocarcinoma of the lung. Eur J Cardiothorac Surg. Jun; 2004 25(6):1102–6. [PubMed: 15145016]
13. Nakata M, Sawada S, Yamashita M, Saeki H, Kurita A, Takashima S, Tanemoto K. Objective radiologic analysis of ground-glass opacity aimed at curative limited resection for small peripheral non-small cell lung cancer. J Thorac Cardiovasc Surg. Jun; 2005 129(6):1226–31. [PubMed: 15942561]
14. Suzuki K, Koike T, Asakawa T, Kusumoto M, Asamura H, Nagai K, Tada H, Mitsudomi T, Tsuboi M, Shibata T, Fukuda H, Kato H. Japan Lung Cancer Surgical Study Group (JCOG LCSSG). A prospective radiological study of thin-section computed tomography to predict pathological

noninvasiveness in peripheral clinical IA lung cancer (Japan Clinical Oncology Group 0201). J Thorac Oncol. Apr; 2011 6(4):751–6. [PubMed: 21325976]

15. Takamochi K, Nagai K, Yoshida J, Suzuki K, Ohde Y, Nishimura M, Sasaki S, Nishiwaki Y. Pathologic N0 status in pulmonary adenocarcinoma is predictable by combining serum carcinoembryonic antigen level and computed tomographic findings. J Thorac Cardiovasc Surg. Aug; 2001 122(2):325–30. [PubMed: 11479506]
16. Nomori H, Ohtsuka T, Naruke T, Suemasu K. Histogram analysis of computed tomography numbers of clinical T1 N0 M0 lung adenocarcinoma, with special reference to lymph node metastasis and tumor invasiveness. J Thorac Cardiovasc Surg. Nov; 2003 126(5):1584–9. [PubMed: 14666037]
17. Jacobs C, van Rikxoort EM, Scholten ET, de Jong PA, Prokop M, Schaefer-Prokop C, van Ginneken B. Solid, part-solid, or non-solid?: classification of pulmonary nodules in low-dose chest computed tomography by a computer-aided diagnosis system. Invest Radiol. Mar; 2015 50(3): 168–73. [PubMed: 25478740]
18. Nakao M, Yoshida J, Goto K, Ishii G, Kawase A, Aokage K, Hishida T, Nishimura M, Nagai K. Long-term outcomes of 50 cases of limited-resection trial for pulmonary ground-glass opacity nodules. J Thorac Oncol. Oct; 2012 7(10):1563–6. [PubMed: 22878750]
19. Yoshida J, Ishii G, Hishida T, Aokage K, Tsuboi M, Ito H, Yokose T, Nakayama H, Yamada K, Nagai K. Limited resection trial for pulmonary ground-glass opacity nodules: case selection based on high-resolution computed tomography-interim results. Jpn J Clin Oncol. Jul; 2015 45(7):677–81. [PubMed: 25900903]
20. Scholten ET, Jacobs C, van Ginneken B, van Riel S, Vliegenthart R, Oudkerk M, de Koning HJ, Horeweg N, Prokop M, Gietema HA, Mali WP, de Jong PA. Detection and quantification of the solid component in pulmonary subsolid nodules by semiautomatic segmentation. Eur Radiol. Feb; 2015 25(2):488–96. [PubMed: 25287262]
21. Son JY, Lee HY, Lee KS, Kim JH, Han J, Jeong JY, Kwon OJ, Shim YM. Quantitative CT analysis of pulmonary ground-glass opacity nodules for the distinction of invasive adenocarcinoma from pre-invasive or minimally invasive adenocarcinoma. PLoS One. Aug 7.2014 9(8)
22. Balagurunathan Y, Gu Y, Wang H, Kumar V, Grove O, Hawkins S, Kim J, Goldgof DB, Hall LO, Gatenby RA, Gillies RJ. Reproducibility and Prognosis of Quantitative Features Extracted from CT Images. Transl Oncol. Feb 1; 2014 7(1):72–87. [PubMed: 24772210]
23. Yanagawa M, Tanaka Y, Leung AN, Morii E, Kusumoto M, Watanabe S, Watanabe H, Inoue M, Okumura M, Gyobu T, Ueda K, Honda O, Sumikawa H, Johkoh T, Tomiyama N. Prognostic importance of volumetric measurements in stage I lung adenocarcinoma. Radiology. Aug; 2014 272(2):557–67. [PubMed: 24708191]
24. Chae HD, Park CM, Park SJ, Lee SM, Kim KG, Goo JM. Computerized texture analysis of persistent part-solid ground-glass nodules: differentiation of preinvasive lesions from invasive pulmonary adenocarcinomas. Radiology. Oct; 2014 273(1):285–93. [PubMed: 25102296]
25. Li Z, Ye B, Bao M, Xu B, Chen Q, Liu S, Han Y, Peng M, Lin Z, Li J, Zhu W, Lin Q, Xiong L. Radiologic Predictors for Clinical Stage IA Lung Adenocarcinoma with Ground Glass Components: A Multi-Center Study of Long-Term Outcomes. PLoS One. Sep 4.2015 10(9):e0136616. [PubMed: 26339917]
26. Maldonado F, Duan F, Raghunath SM, Rajagopalan S, Karwoski RA, Garg K, Greco E, Nath H, Robb RA, Bartholmai BJ, Peikert T. Noninvasive Computed Tomography-based Risk Stratification of Lung Adenocarcinomas in the National Lung Screening Trial. Am J Respir Crit Care Med. Sep 15; 2015 192(6):737–44. [PubMed: 26052977]
27. Maldonado F, Boland JM, Raghunath S, Aubry MC, Bartholmai BJ, Deandrade M, Hartman TE, Karwoski RA, Rajagopalan S, Sykes AM, et al. Noninvasive characterization of the histopathologic features of pulmonary nodules of the lung adenocarcinoma spectrum using computer-aided nodule assessment and risk yield (CANARY)—a pilot study. J Thorac Oncol. 2013; 8:452–460. [PubMed: 23486265]
28. Raghunath S, Maldonado F, Rajagopalan S, Karwoski RA, DePew ZS, Bartholmai BJ, Peikert T, Robb RA. Noninvasive risk stratification of lung adenocarcinoma using quantitative computed tomography. J Thorac Oncol. 2014; 9:1698–1703. [PubMed: 25170645]

Central Message

The **C**omputer **A**ided **N**odule **A**ssessment and **R**isk **Y**ield (CANARY) tool provides a validated approach for non-invasive lung nodule risk stratification.

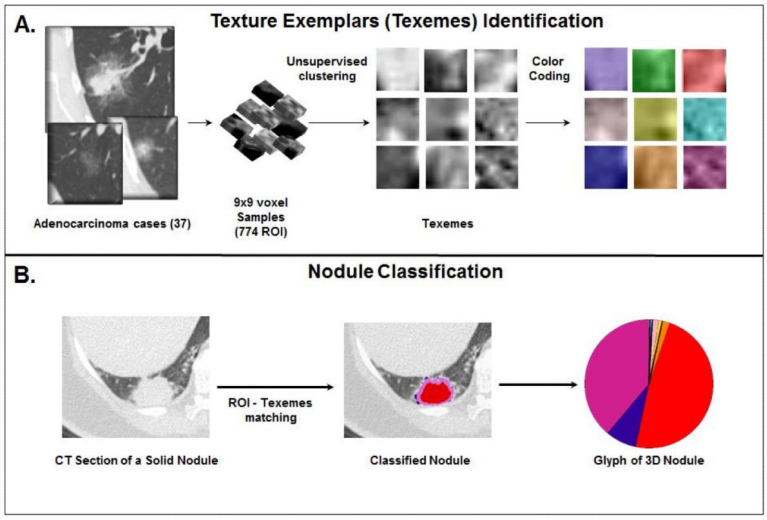

Figure 1.

(A) CANARY pattern identification. Based on arbitrarily selected 774 9×9 regions of interest (ROI) from 37 lung adenocarcinoma nodules, nine natural clusters were identified. The most “central” ROI of each cluster was selected as the cluster’s texture exemplar and the exemplars were color-coded. (B) When processing a new nodule, each voxel and its surrounding ROI is compared to the nine exemplars (texemes) and the voxel is color coded to the nearest texeme. The relative distribution of the texemes is displayed in a glyph.

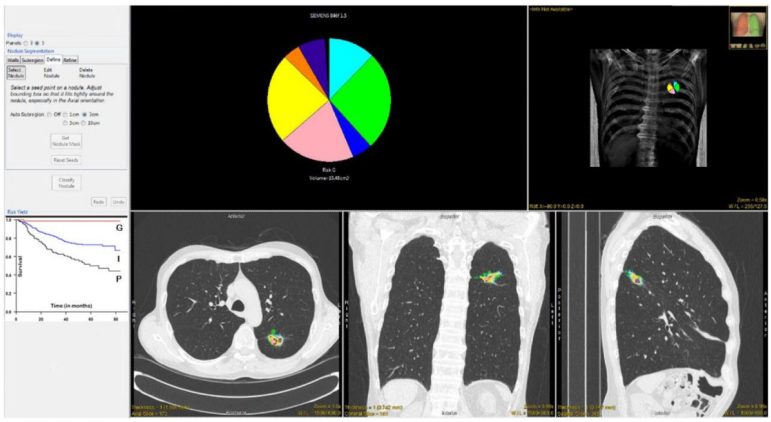

Figure 2.

CANARY user interface. The CANARY results are overlaid on representative orthogonal CT sections. The glyph and the associated risk group provides a succinct overview of the nodule. Kaplan-Meier curves for the risk groups are provided as reference.

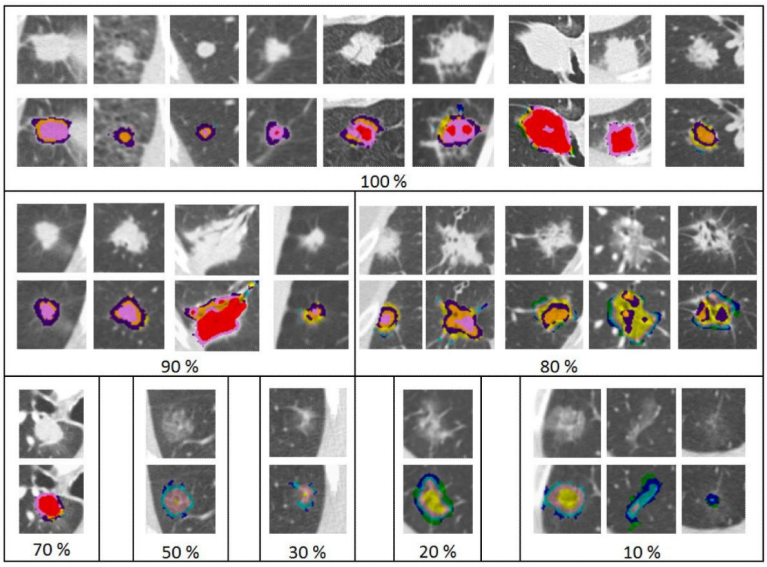

Figure 3.

Radiologic–histopathologic correlation of tissue invasion between CANARY-based nodule assessment and consensus histopathology. Selected adenocarcinoma nodules are displayed above their superimposed CANARY signatures. Nodules are grouped according to degree of histologic invasion specified in % within each panel.

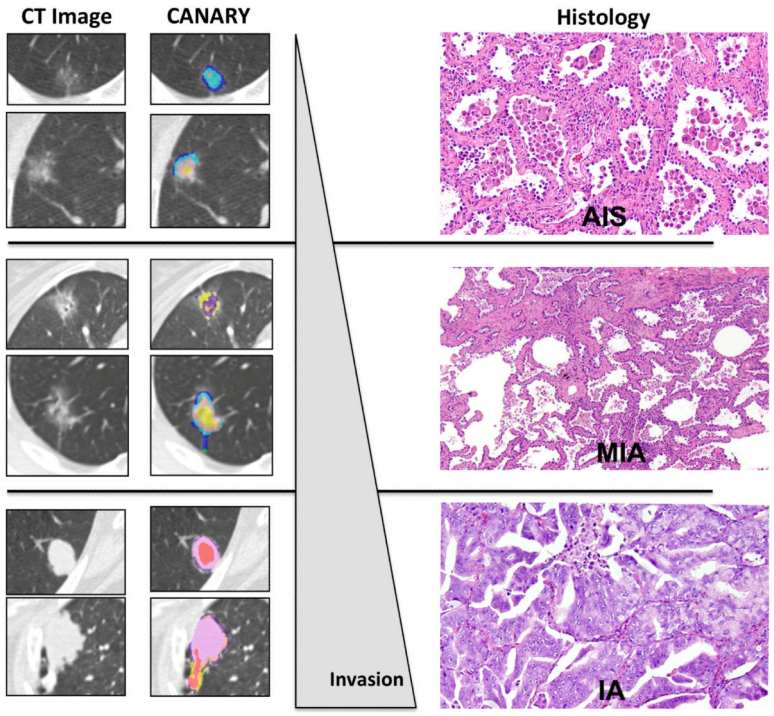

Figure 4.

CANARY facilitates Radiological-Pathological correlation. Column 1 shows representative axial HRCT slices of representative lung nodules. Column 2 displays the corresponding CANARY analysis of these nodules, which by consensus histology were identified as adenocarcinoma in situ (AIS), minimally invasive adenocarcinoma (MIA) or invasive adenocarcinoma (IA), respectively. Column 3 shows histological examples of AIS, MIA and IA.

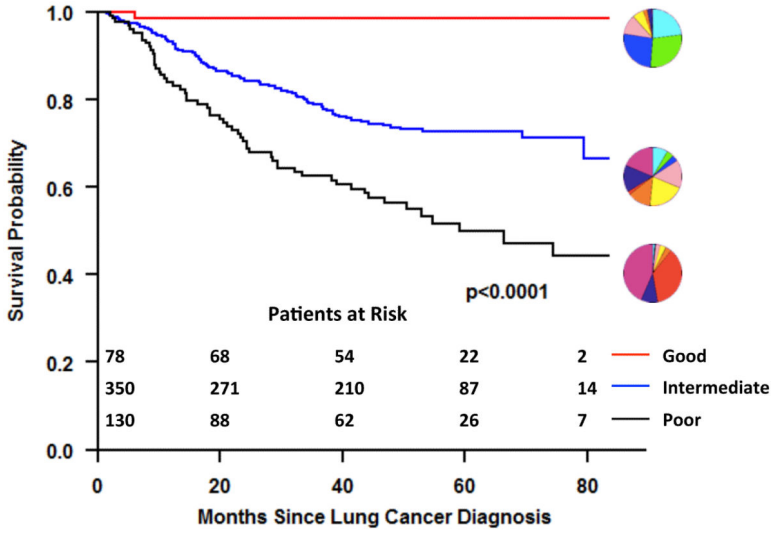

Figure 5.

CANARY analysis allows the non-invasive risk stratification of lung adenocarcinomas. Kaplan Meier analysis of the progression free survival, for 558 patients (264 Mayo Clinic cohort and 294 NLST study) with lung adenocarcinoma based on the CANARY risk groups (G=good, I=intermediate and P=poor). (28,26) The glyphs displayed in conjunction with each curve represent the exemplar glyph for the corresponding CANARY risk group

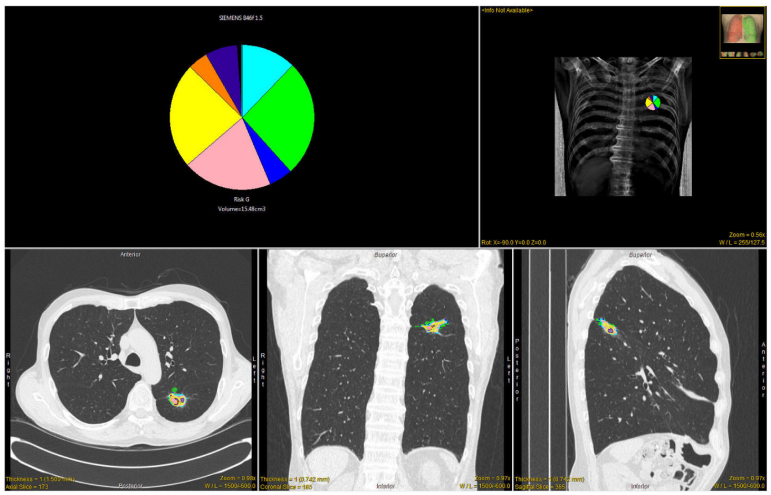

Central Picture.
CANARY: Validated, clinically relevant non-invasive lung nodule risk stratification.